

Ensemble based convergence assessment of biomolecular trajectories

Edward Lym an,¹ and Daniel M. Zuckerman²

July 1, 2019

Abstract

Assessing the convergence of a biomolecular simulation is an essential part of any computational investigation. This is because many important quantities (e.g., free energy differences) depend on the relative populations of different conformers; insufficient convergence translates into systematic errors. Here we present a simple method to self-consistently assess the convergence of a simulation. Standard clustering methods first generate a set of reference structures to any desired precision. The trajectory is then classified by proximity to the reference structures, yielding a one-dimensional histogram of structurally distinct populations. Comparing ensembles of different trajectories (or different parts of the same trajectory) built with the same reference structures provides a sensitive, quantitative measure of convergence. Please note: this is a preliminary manuscript, and should be read as such. Comments are most welcome, especially regarding pertinent prior work.

1 Introduction

Conformational fluctuations are essential to the function of proteins, whether they are motor proteins[1], enzymes[2,3], signalling proteins[4,5], or almost any other. Different experiments allow observation of protein fluctuations

¹elyman@ccb.pitt.edu

²dmz@ccb.pitt.edu

over a huge range of time scales, from picoseconds[6] to microseconds[5] to milliseconds[3,7] to seconds and longer[8].

Naturally then, simulations aim to observe conformational fluctuations as well. A gap remains, however, between the time scale of any biologically important motions (sec/sec), and that accessible to atomically detailed simulation (nsec). To put it another way, some problems are simply not possible to study computationally, since it is so far impossible to run a simulation which is long enough."

For those problems which are at the very edge of being feasible, we would like to know whether we have indeed sampled enough to draw quantitative conclusions. These problems include the calculation of free energies of binding[], ab initio protein folding[9,10], and simulation of flexible peptides[11] and conformational changes.

Convergence assessment is also crucial for rigorous tests of simulation protocols and empirical force fields. Many algorithms propose to improve the sampling of conformation space, but quantitative estimation of this type of efficiency is difficult. In the case of force field validation, it is important to know whether systematic errors are a consequence of the force field, or are due to undersampling.

The observed convergence of a simulation depends on how convergence is defined and measured. It is therefore important to consider what sort of quantity is to be calculated from the simulation, and choose an appropriate way to assess the adequacy of the simulation trajectory (or trajectories). Many methods relatively simple are commonly used, such as measuring distance from the starting structure as a function of simulation time, and calculation of various autocorrelation functions[12,13]. Other, more sophisticated methods are based on principal components[14,15] or calculation of energy-based ergodic measures[16].

Many applications, however, require a thorough and equilibrated sampling of the space of structures. All of the methods just listed are only related indirectly to structural sampling. For example, there are many examples of groups of structures which are very close in energy, but very dissimilar structurally. In such cases, we might expect energy-based methods to be insensitive to the relative populations of the different structural groups. It is therefore of interest to develop methods which are more directly related to the sampling of different structures, and see how such methods compare to more traditional techniques.

Other authors have previously considered convergence assessment by count-

ing structural clusters. Daura et. al. developed a method which assigns clusters based upon a cutoff in the RMSD metric[17,18]. The authors then assess the convergence of a simulation by considering the number of clusters as a function of time. Convergence is deemed sufficient when the curve plateaus. This is surely a better measure than simpler, historically used methods, such as RMSD from the starting structure or the running average energy. However, it is worth noting that long after the curve of number of clusters vs. time plateaus, the populations of the clusters may still be changing. Indeed, an important conformational substate which has been visited just once will appear as a cluster, but its relative population will certainly not have equilibrated.

The method of Daura et. al. also suffers from the need to store the entire matrix of pairwise distances. For a trajectory of length N , the memory needed scales as N^2 , rendering the method impractical for long trajectories. At least two groups have developed methods which rely on nonhierarchical clustering schemes, and therefore require memory which is only linear in N . Karpen et. al. developed a method which optimizes the clusters based on distance from the cluster center[19], with distances measured in dihedral angle space. Elmer and Pande have optimized clusters subject to a constraint on the number of clusters[20], with distance defined by the atom–atom distance root mean square deviation[21,22]. We will simply select reference structures at random from the trajectory, but ensure that all reference structures are separated by a (user-defined) minimum distance.

In this paper, we address systematically the measurement of sampling quality. Our method classifies (or bins) a trajectory based upon the “distances” between a set of reference structures and each structure in the trajectory. Our method is unique in that it not only builds clusters of structures, it also compares the cluster populations. By comparing different fragments of the trajectory to one another, convergence of the simulation is judged by the relative populations of the clusters. We believe the key to assessing convergence is tracking relative bin populations.

In the next section, we present a detailed description of the algorithm and discuss possible choices of metric. We then demonstrate the method on simulations of met-enkephalin, a structurally diverse peptide.

2 Theory and methods

We will evaluate sampling by comparing "structural histograms", to be described below. These histograms provide a fingerprint of the conformation space sampled by a protein, by projecting a trajectory onto a set of reference structures. Comparing histograms for different pieces of a trajectory (or for two different trajectories), projected onto the same set of reference structures, provides a very sensitive measure of convergence. Not only are we comparing how broadly has each trajectory sampled conformation space, but also how frequently each substate has been visited.

2.1 Histogram construction

We generated the set of reference structures and corresponding histogram in the following simple way (our choice for measuring conformational distance will be discussed below):

- (i) A cutoff distance d_c is defined.
- (ii) A structure S_1 is picked at random from the trajectory.
- (iii) S_1 and all structures less than d_c from S_1 are removed from the trajectory.
- (iv) Repeat (ii) and (iii) until every structure is clustered, generating a set S of reference structures.
- (v) The set S of reference structures is then used to build a histogram, by grouping each frame with its nearest reference structure.

Such a partitioning guarantees a set of clusters whose centers are at least d_c apart. Furthermore, for a trajectory of N frames, the number of M reference structures, and therefore the memory needed to store the resulting $M \times N$ matrix of distances, is controlled by d_c . For physically reasonable cutoffs (e.g., $d_c \approx 1 \text{ \AA}$), the number of reference structures is at least an order of magnitude smaller than the number of frames in the trajectory. The memory requirements are therefore manageable, and the computation of pairwise distances scales as $N \log N$.

There is nothing in principle which prevents the use of a more carefully chosen set of reference structures with our convergence assessment method. For example, we may consider a set of structures which correspond to minima of the potential energy surface. The cutoff would then be chosen to be the smallest observed distance between any pair of the minimum energy

structures, and the set of reference structures so determined would be augmented by the random selection of more references in order to span the whole trajectory.

However, we expect that the purely random selection used here will naturally find the lowest free energy (i.e., most populated) structures. In either case, any set of reference structures defines a unique histogram for any trajectory.

Once we have a set of reference structures, we may easily compare two different trajectories classified by the same set of reference structures, by comparing the populations of the various bins as observed in the two trajectories: given a (normalized) population $p_i(1)$ for cluster i in the first trajectory, and $p_i(2)$ in the second, the difference in the populations $P_i = p_i(1) - p_i(2)$ measures the convergence of substate i 's population between the two trajectories.

Note that the "two" trajectories just discussed may be two different pieces of the same simulation. In this way, we may self-consistently assess the convergence of a simulation, by looking to see whether the relative populations of the most populated substates are changing with time. Of course, this cannot answer affirmatively that a simulation has converged (no method can do so), however, it may answer negatively. In fact, we will see later that our method indicates that structural convergence is much slower than previously appreciated.

2.2 Metrics

Many different metrics have been used to measure distance between conformations. The choice depends on both physical and mathematical considerations. For example, dihedral angle based metrics are well-suited to capture local structural information [19], but are not sensitive to more global rearrangements of the molecule. Least-squares superposition followed by calculation of the average positional fluctuation per atom (RM SD) is quite popular, but the problem of optimizing the superposition can be both subtle and time-consuming for large, multi-domain proteins [23]. In addition, RM SD does not satisfy a triangle inequality [24]. This is not an issue for the algorithm presented here, but is a consideration for more sophisticated clustering methods [20]. We will use RM SD to measure distance here, though we note that "distance root mean square deviation" (dRMS) (or sometimes, "distance matrix error") [21,22] may be appropriate when RM SD is not.

Labelling the two structures by a and b , the traditional root mean square deviation (RM SD) is defined to be the minimum of

$$\text{RM SD } (a; b) = \sqrt{\frac{1}{N} \sum_{j=1}^N \| \mathbf{x}_j^a - \mathbf{x}_j^b \|^2}; \quad (1)$$

where N is the number of atoms and \mathbf{x}_j is the position of atom j in the aligned frame.

2.3 Choice of cut-off

It is clear that the choice of d_c , together with the choice of metric, determines the resolution of the histogram. Reducing d_c increases the number of reference structures, and reduces the size of the bins. How is d_c chosen? There is no general answer, the cut-off will depend on the problem under investigation. If the magnitude of some important conformational change is known in advance, then this information will guide the selection of an appropriate cut-off. If not, then a series of histograms ought to be constructed at various d_c 's. The behavior of the histogram as a function of d_c will give a sense of the appropriate value, as we will see below.

3 Results

We have tested our classification algorithm on implicitly solvated met-enkephalin, a pentapeptide neurotransmitter. By focusing first on a small peptide, we aim to develop the methodology on a system which may be thoroughly sampled and analyzed by standard techniques. In addition to comparing our ensemble method to other techniques, we will compare ensembles based on RM SD classification, to those based on the RMS metric.

The trajectories analyzed in this section were generated by Langevin dynamics simulations, as implemented in the Tinker v. 4.2.2 simulation package [25]. The temperature was 298 K, friction constant was 5 ps⁻¹, and solvation energy was treated by the GB/SA method [26]. Two 100 nsec trajectories were generated, each starting from the PDB structure 1plw, model 1. The trajectories will be referred to as plw-a and plw-b. Coordinates were written every 10 psec, for a total of 2 × 10⁴ frames per trajectory.

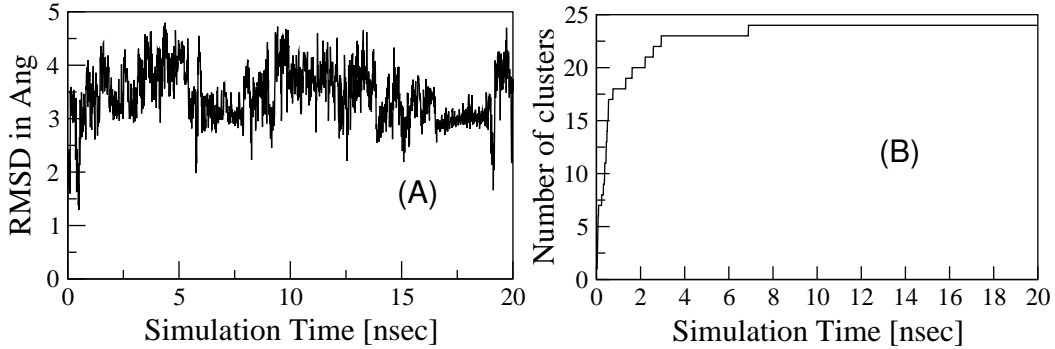


Figure 1: (A) RM SD from starting structure for met-enkephalin trajectory plw-a. (B) Number of populated clusters vs. simulation time for the plw-a trajectory. After 7 nsec, the simulation appears equilibrated. No more clusters appear in the 198 nsec plw-ab trajectory.

An often used indicator of equilibration is the RM SD from the starting structure (see g. 1A). Such plots are motivated by the recognition that the starting structure (e.g., a crystal structure) may not be representative of the protein at the simulation conditions (e.g., native conditions). This is clearly the case in g. 1A, as the computation was performed with an implicit water model, and the experimental structure was determined in the presence of bicelles[27]. The system fails to settle down to a relatively constant distance from the starting structure; rather, it is moving between various substates, some nearer and some farther from the starting structure. While this is not surprising for a peptide renowned for its floppy character, it also indicates that this method cannot determine when the peptide simulation has converged. Indeed, g. 1A can tell us nothing about the convergence of the simulation, only that it spends most of its time more than 2.0 Å from the starting structure.

A perhaps better indication of equilibration is provided by g. 1B, in which we have used the method of Daura, et. al[7], albeit with clusters built by the procedure described in sec. 2.1. The premise is that convergence is achieved when the number of clusters no longer increases, as this means that the simulation has visited every substate. This analysis suggests that convergence is observed by about 7 nsec, and the curve has the comforting appearance of saturation. However, g. 1B is insensitive to the relative populations of the clusters. To illustrate the problem, consider a simple potential,

| d_c in A | number of clusters (d_c in RM SD) | |
|------------|--------------------------------------|-----|
| 1.5 | | |
| 2.0 | | |
| 2.5 | 72.8 | 3.8 |
| 3.0 | 23.3 | 2.2 |
| 3.5 | 10.3 | 0.5 |

Table 1: Number of reference structures generated for various cuts (d_c in RM SD). Reported are the average and standard deviation in the number of reference structures for four independent clustering runs of the plw-ab trajectory.

with two smooth wells separated by a high barrier. By e.g. ??B, a simulation will be converged as soon as it has crossed the barrier once. It is clear, however, that many crossings will be required before the populations of the two states have equilibrated. (This was mentioned by Daura et. al. in ref.??.) We will address this question using our ensemble-based method. We find, in fact, that the relative populations of the clusters continue to change, long after their number has equilibrated.

3.1 Ensemble based comparison of trajectories

3.1.1 Reference structure generation and cut selection

A compound trajectory was formed from trajectories plw-a and plw-b, by discarding the first 1 nsec of each trajectory and concatenating the two into a single, 198 nsec trajectory (plw-ab). We then generated a set of reference structures for the compound trajectory, as described earlier: a structure is picked at random, and it is temporarily discarded along with every structure within a predefined cut-off distance, d_c . The process is repeated on the remaining structures until the trajectory has been exhausted. The result is a set of reference structures which are separated from one another by at least the predefined cut-off distance. Lowering the cut-off (making the reference structures more similar) increases the resolution of the clustering, and increases the number of reference structures (see table 1). While RM SD is system-size dependent [28], for a particular system the cut-off defines a resolution.

The dependence of the histogram on d_c is shown in Fig. 2. With $d_c = 3.0$

At the first three bins already account for more than 50% of the total population. It might be expected that such a coarse description of the ensemble may not be particularly informative; however, we will see in the next sections that this level is already sufficient to make powerful statements about convergence.

Lowering the cutoff, the general features of the histogram remain unchanged: a steep slope initially, which accounts for half of the total population, followed by a flatter region. In each case, most (90%) of the population is accounted for by approximately half of all the reference structures. However, a closer inspection reveals that the fraction of bins required to account for the noted percentages of population (50, 75, and 90%) is decreasing with the cutoff | although the differences between the 2.0 and 1.5 Å data are very slight.

Though we do not pursue it here, we note that the tail of the distribution | where half of all the bins account for only 10% of the population | might contain some very interesting structures. Indeed, at the very end of the tail are found bins which sometimes contain a single structure. Might some of these low population bins represent transition states? For now, we set this question aside, and focus instead on convergence assessment.

3.1.2 Comparing trajectories to a "gold standard" ensemble

In some applications, we want to compare a trajectory to a "gold standard" ensemble. For example, the gold standard might be the ensemble sampled by a long molecular dynamics simulation, and we may wish to check the ensemble produced by a new simulation protocol against the long molecular dynamics trajectory.

Once a set of references is calculated, an ensemble is built by grouping each frame in a trajectory with its nearest reference structure. Carrying out this procedure on the entire 198 nsec compound trajectory orders the reference structures, as in figure 3, where we used a cutoff of 3.0 Å RMSD. We can then assess the convergence of portions of the trajectory against this full ensemble (see figs. 3A-D).

From fig. 3A, it is clear that after the first 2 nsec, the simulation is far from converged. Many important substates have not yet been visited, and many of the populations are over or underpopulated by several $k_B T$. (On a semi-log scale, a factor of 2 in the population represents an error of approximately $1=2 k_B T$.) After 50 nsec (fig. 3(C)), all clusters are populated, but many

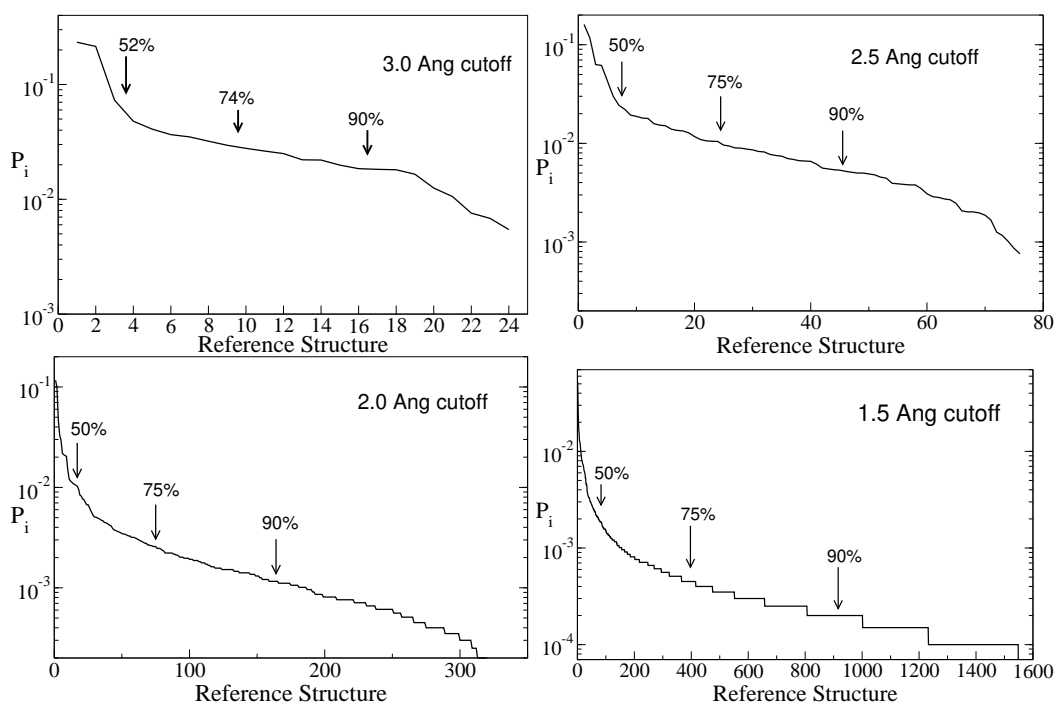


Figure 2: caption here

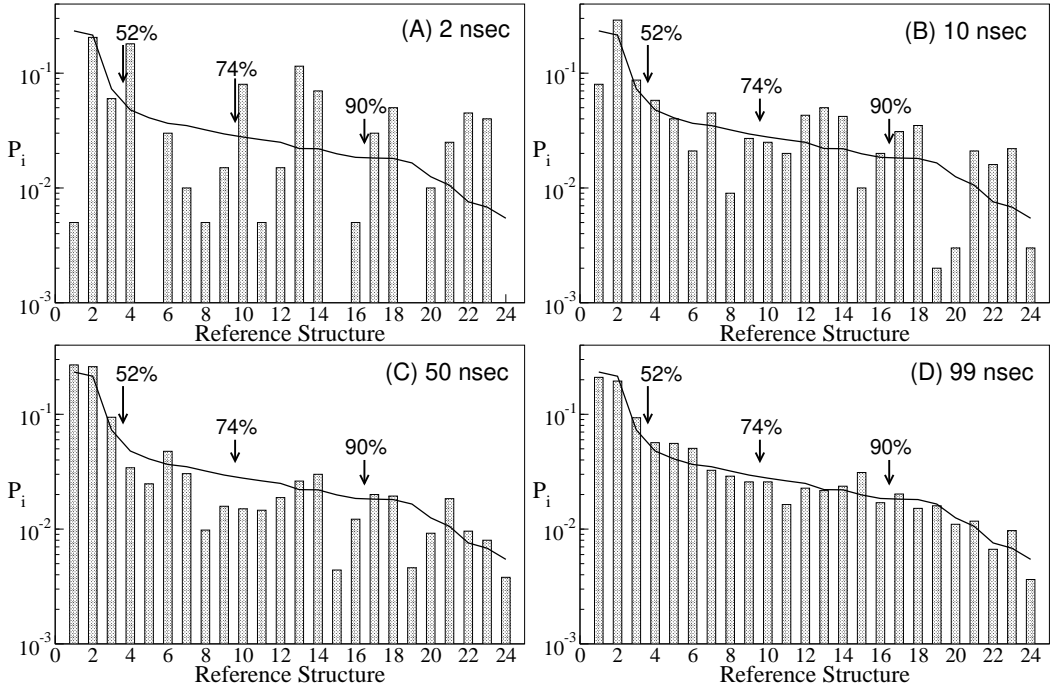


Figure 3: Ensembles for diereent fractions of trajectory *plw-a* (bars), compared to the ensemble of the entire 198 nsec compound trajectory (solid line): 2 nsec (A), 10 nsec (B), 50 nsec (C), 99 nsec (D). $d_c = 3.0 \text{ \AA RM SD}$. Note that $\ln P_i$ is a free-energy like quantity; hence on the semilog scale the diereence in populations may be read in units of $k_b T$: a factor of 2 on the y-axis corresponds to $0.5 k_b T$. The percentages indicate the fraction of the 198 nsec trajectory binned to that point.

important substates have not converged to within $1=2 k_B T$ of the 198 nsec values.

Fig. 3 presents a picture of a very conformationally diverse peptide. The first 3 substates contain only 52% of the observed structures, while the first 9 account for 74%. Indeed, the (experimentally determined) starting structure is located in the second most populated substate.

The experimental structure was determined in the presence of bicelles, as it was hypothesized that interaction of the peptide with the cell membrane induces a shift in the conformational distribution [27]. We therefore classified the entire set of 80 NMR structures against our set of reference structures. The overwhelming majority of the NMR structures (75%) were nearest to reference number 23, the second-least populated bin in our simulation. The next largest group of NMR structures (15 of 80) were nearest to reference number 2, which held a comparable portion of the simulation trajectory. The remaining 5 NMR structures were scattered among 4 different bins. While not conclusive, the comparison between our simulation data and the NMR structures supports the hypothesis that binding to the membrane induces a shift in the distribution of met-enkephalin conformers. While such conformational diversity is not surprising for a peptide, which is known to be a promiscuous neurotransmitter by virtue of its flexibility [27,29,30], it will be interesting to revisit the issue in the study of a protein.

3.2 Convergence Assessment

Fig. 3 is the sort of plot that might be used to compare simulation protocols: ensembles from a new protocol may be compared to a "gold-standard" ensemble. (Here, the gold standard is the 198 nsec compound trajectory.) However, it is not useful as a means of assessing the convergence of a simulation. After all, given only a 4 nsec trajectory, one must attempt an assessment without reference to "the answer". Instead, we can only compare, for example, the first 2 nsec to the second 2 nsec, as in Fig. 4A. The series of figures in Fig. 4 shows that the populations of the clusters are still changing significantly, even between the first and second 50 nsec. Presuming we had run only a single 100 nsec simulation, we could make Fig. 4C, and sum up the convergence by saying, "at a resolution of 3.0 Å RM SD, considering bins containing 75% of the structures, 6 of 9 bins have not yet converged to within $1=2 k_B T$." Note the contrast with Fig. 1B, where it appears convergence is reached after just 7 nsec.

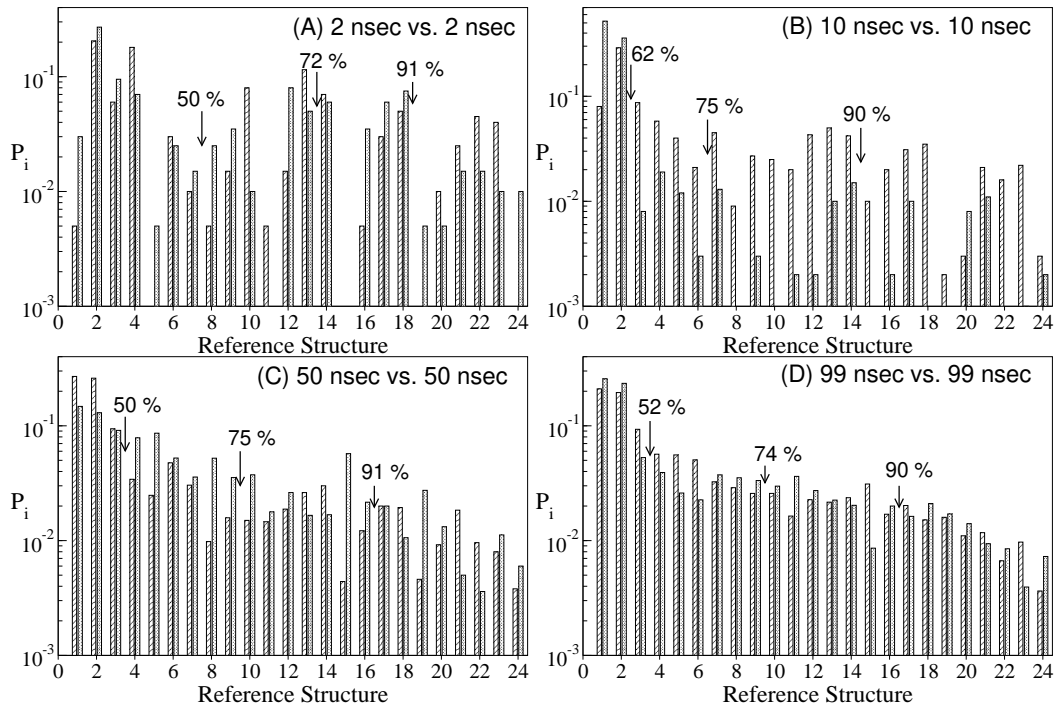


Figure 4: Self-consistent convergence of different trajectory lengths. Each plot compares the first half (diagonal hatching) to the second half (gray shading) of the trajectory for total trajectory lengths of (A), 4 nsec; (B), 20 nsec; (C), 100 nsec; (D), 198 nsec. Percentages indicate the portion of the total trajectory binned to that point.

| block length | number of pairs | \bar{P}_i | P |
|--------------|-----------------|-------------|-------|
| 2 nsec | 36 | 0.557 | 0.208 |
| 10 nsec | 36 | 0.402 | 0.133 |
| 20 nsec | 36 | 0.302 | 0.080 |
| 49.5 nsec | 6 | 0.295 | 0.070 |

Table 2: Histogram comparisons for different block lengths. The quantity P is calculated according to equation 2, and then averaged over a number of different pairs of blocks, given in column 2. The standard deviation of the set of pairs is given in column 4.

Fig. 4 provides a nice visual summary of the convergence of a simulation, however, we would like to be able to compare different plots, which may not be easily distinguished by eye. We therefore define a quantity $P(a;b)$, which measures the difference between histograms for two trajectories, labeled ‘‘a’’ and ‘‘b’’:

$$P(a;b) = \frac{1}{2} \sum_{i=1}^{N^2} |P_i(a) - P_i(b)| \quad (2)$$

where P_i is the population of bin i , and the sum runs over the N^2 bins. The factor 1/2 accounts for the fact that two trajectories are compared, so that $P(a;b)$ is bounded by 0 (identical trajectories), and 1 (no populated bins in common).

In answer to the question ‘‘is my simulation well-converged?’’, plots like those in fig. 4 are able to unambiguously answer only, ‘‘No.’’ An apparently positive answer, as suggested by fig. 4D, may simply represent a fortuitous moment in a still-relaxing simulation. We therefore consider whether the histograms in fig. 4 are representative of the typical pair.

To this end, we have computed P for several pairs of histograms (table 2). The trend from 2 nsec to 20 nsec blocks is clear: both P and its variance decrease, indicating the simulation is better converged, as we would expect.

The observed ensembles and corresponding P ’s depend on both the metric used and the value of d_c . (This is of course true of any clustering algorithm.) It is therefore important to report this information along with any statements about the convergence of a particular simulation. Indeed, lowering the $cutoff$, and hence increasing the resolution of the classification, is bound to reduce the observed level of convergence. Instead of fig. 3, in which

each panel is a different length of the trajectory, we could have plotted the same trajectory length at different resolutions. At a high enough resolution, we will always find some substates which are under- or over-populated. In other words, since all trajectories are finite, a physically acceptable value of d_c must be chosen.

4 Discussion

The results for met-enkephalin indicate that it takes quite some time for the relative populations of the various substates to equilibrate. This makes sense; after all, a single substate will appear on a plot such as Fig. 1B after having been visited only once. However, we can expect that many transitions into and out of each substate will be required to equilibrate their relative populations.

In order to carefully assess convergence of a simulation, we must therefore compare the populations of the various substates from different fragments of the trajectory. A simple, fast way to carry out such a comparison is provided by the comparative ensemble method described above. A higher level of rigor can be achieved by comparing multiple pairs of independent blocks of the trajectory.

It must be stressed that though our method may provide an unambiguous negative answer to the question, "Is the simulation converged?" it may only provide a provisionally positive answer. A longer simulation may well reveal longer time scale phenomena, parts of structure space not yet visited.

We hope that this method will find application especially in the area of simulation efficiency evaluation. Many algorithms have recently generated broad interest by virtue of their potential to enhance the sampling of biomolecular conformation space. Some of these algorithms, notably the various parallel exchange simulations[31], invest considerable CPU time in pursuit of this goal. It is therefore important to ask whether these methods are in fact worth the extra expense, i.e., "does running the algorithm in question increase the quantity: (observed conformational sampling) / (total CPU time)"? The CPU time is easy enough to quantify, and we hope the present report will aid in evaluating the numerator.

References

- [1] Karel Svoboda, Partha P. Mitra, and Steven M. Block. Fluctuation analysis of motor protein movement and single enzyme kinetics. *Proc. Nat. Acad. Sci. USA*, 91:11782{11786, 1994.
- [2] S. A. Mccallum, T. K. Hitchens, C. Torborg, and G. S. Rule. Ligand induced changes in the structure and dynamics of a human class mu glutathione s transferase. *Biochemistry*, 39:7343{7356, 2000.
- [3] Elan Zohar Eisenmesser, Daryl A. Bosco, Michael A. Kue, and Dorothy E. Kern. Enzyme dynamics during catalysis. *Science*, 295:1520{1523, 2002.
- [4] Mingjie Zhang, Toshiyuki Tanaka, and Mitsuhiro Ikura. Calcium induced conformational transition revealed by the solution structure of apo calmodulin. *Nature Struct. Biol.*, 2:758{767, 1995.
- [5] Brian F. Volkman, Doron Lipson, David E. Wemmer, and Dorothy E. Kern. Two-state allosteric behavior in a single-domain signaling protein. *Science*, 291:2429{2433, 2001.
- [6] Friedrich Schotte, Manho Lim, Timothy A. Jackson, Aleksandr V. Smirnov, Jayashree Soman, John S. Olson, George N. Phillips Jr., Michael Wulff, and Phillip A. Arnsdorf. Watching a protein as it functions with 150{ps time{resolved X-ray crystallography. *Science*, 300:1944{1947, 2003.
- [7] Ryoko Itahara, Shigeyuki Yokoyama, and Kazuyuki Kasaka. NMR snapshots of a fluctuating protein structure: Ubiquitin at 30 bar/3 kbar. *J. Mol. Biol.*, 347:277{285, 2005.
- [8] Michele Vendruscolo, Emanuele Paci, Christopher M. Dobson, and Martin Karplus. Rare fluctuations of native proteins sampled by equilibrium hydrogen exchange. *J. Am. Chem. Soc.*, 125:15686{15687, 2003.
- [9] Philip Bradley, Kira M. S. Misra, and David Baker. Toward high-resolution de novo structure prediction for small proteins. *Science*, 309:1868{1871, 2005.
- [10] Carlos Simmerling, Bentley Strockbine, and Adrian E. Roitberg. All-atom structure prediction and folding simulations of a stable protein. *J. Am. Chem. Soc.*, 124:11258{11259, 2002.

[11] Min-Yi Shen and Karl F. Freed. Long time dynamics of met-enkephalin: comparison of explicit and implicit solvent models. *Biophys. J.*, 82:1791–1808, 2002.

[12] M. H. Zaman, M.-Y. Shen, R. S. Berry, and K. F. Freed. Computer simulation of met-enkephalin using explicit atom and united atom potentials: similarities, differences and suggestions for improvement. *J. Phys. Chem.*, 107:1686–1691, 2003.

[13] Wei Zhang, Chun Wu, and Yong Duan. Convergence of replica exchange molecular dynamics. *J. Chem. Phys.*, 123:154105(1–154105(9, 2005.

[14] Berk Hess. Convergence of sampling in protein simulations. *Phys. Rev. E* 65:031910(1–031910(10, 2002.

[15] K. Y. Sanbonmatsu and A. E. Garcia. Structure of met-enkephalin in explicit aqueous solution using replica exchange molecular dynamics. *PROTEINS*, 46:225–234, 2002.

[16] John E. Straub, Alissa B. Rashkin, and D. Thirumalai. Dynamics in rugged energy landscapes with applications to the S-peptide ribonuclease A. *J. Am. Chem. Soc.*, 116:2049–2063, 1994.

[17] Xavier Daura, Wilfred F. van Gunsteren, and Alan E. Mark. Folding-unfolding thermodynamics of a heptapeptide from equilibrium simulations. *PROTEINS*, 34:269–280, 1999.

[18] Lorna J. Smith, Xavier Daura, and Wilfred F. van Gunsteren. Assessing equilibration and convergence in biomolecular simulations. *PROTEINS*, 48:487–496, 2002.

[19] Mary E. Karpen, Douglas J. Tobias, and Charles L. III Brooks. Statistical clustering techniques for the analysis of long molecular dynamics trajectories: analysis of 2.2-ns trajectories of YPGDV. *Biochem.*, 32:412–420, 1993.

[20] Sidney P. Eller and Vijay S. Pande. Foldamer simulations: novel computational methods and applications to poly-phenylacetylene oligomers. *J. Chem. Phys.*, 121:12760–12771, 2004.

[21] K .N ishikawa and T .O oi. Tertiary structure of a protein ii. freedom of dihedral angles and energy calculations. *J. Phys. Soc. Japan*, 32:625{634, 1972.

[22] M ichael Levitt. A simplified representation of protein conformations for rapid simulation of protein folding. *J. Mol. Biol.*, 104:59{107, 1976.

[23] D avid A . Snyder and G aetano T . M ontelione. C lustering algorithms for identifying core atom sets and for assessing the precision of protein structure ensembles. *PROTEINS*, 59:673{686, 2005.

[24] G ordon M .C rippen and Y osiakiZenm aio hikubo. Statistical mechanics of protein folding by exhaustive enumeration. *PROTEINS*, 32:425{437, 1998.

[25] J. W . Ponder and F . M . R ichard. A n efficient newton-like method for molecular mechanics energy minimization of large molecules. *J. Comput. Chem.*, 8:1016{1024, 1987. <http://dasher.wustl.edu/tinker/>.

[26] W . C . Still, A . Tempczyk, and R . C . Hawley. Semianalytical treatment of solvation from molecular mechanics and dynamics. *J. Am. Chem. Soc.*, 112:6127{6129, 1990.

[27] Isabelle M arcotte, Frances Separovic, M ichèle Auger, and Stéphane M . G angé. A multidimensional ^1H NMR investigation of the conformation of methionine enkephalin in fast-tumbling bicelles. *Biophys. J.*, 86:1587{1600, 2004.

[28] V ladimir N .M aiorov and G ordon M .C rippen. Significance of root-mean-square deviation in comparing three-dimensional structures of globular proteins. *J. Mol. Biol.*, 235:625{634, 1994.

[29] N .P .P lotnikov, R .E .Faith, A .J .M urgo, and R .A .G ood. Enkephalins and endorphins: stress and the immune system . Plenum, New York, 1986.

[30] W .H .G raham, E .S .C arter II, and R .P .H icks. Conformational analysis of met-enkephalin in both aqueous solution and in the presence of sodium dodecyl sulfate micelles using multidimensional NMR and molecular modeling. *Biopolymers*, 32:1755{1764, 1992.

[31] Dietmar Paschek and Angel E. Garcia. Reversible temperature and pressure denaturation of a protein fragment: A replica exchange molecular dynamics simulation study. *Phys. Rev. Lett.*, 93:238105{1{238105{4, 2004.